arXiv:2506.17396 / ApJ 989, 209 (2025)

The JWST/AURORA Survey: Multiple Balmer and Paschen Emission Lines for Individual Star-forming Galaxies at $z = 1.5 - 4.4$. I. A Diversity of Nebular Attenuation Curves and Evidence for Non-Unity Dust Covering Fractions

Naveen A. Reddy,[1] Alice E. Shapley,[2] Ryan L. Sanders,[3] Michael W. Topping,[4] Richard S. Ellis,[5] Max Pettini,[6] Gabriel Brammer,[7,8] Fergus Cullen,[9] Natascha M. Förster Schreiber,[10] Ali A. Khostovan,[3] Derek J. McLeod,[9] Ross J. McLure,[9] Desika Narayanan,[11,12] Pascal A. Oesch,[13,7,8] Anthony J. Pahl,[14] Charles C. Steidel,[15] and Danielle A. Berg[16]

1.Introduction

Stellar attenuation curve contains
- Dust absorption /scatter
- Scattering of light into the line of sight
- Nonuniform distribution of column densities
- Spatial variation in optical depth within galaxies

Nebular attenuation curve only capture dust attenuation towards the most massive stars (towards most dusty regions)
(O-Type stars are typically embedded in molecular clouds)
=> stellar and nebular attenuation curve may differ
- Nebular attenuation curve in rest-optical is similar to Galactic curve (Cardelli+89)
- PaB decrements in z<0.3 galaxies show diversity in attenuation curve slopes and normalization (Prescott+22)

2.Data

AURORA (The Assembly of Ultradeep Observations Revealing Astrophysics)
- 46/51 galaxies in COSMOS and G-N => 8 AGN and QGs / 9 bad calibration / 2 inconsistent line ratios with case B / 4 negligible extinction / 34 no coverage of Pa lines targets are removed => 24 galaxies having ~11 lines of Balmer/Pa lines
- R=1000 spec at 1-5um
- z>1.4 auroral emission lines (O, S, N) to measure Te => [O/H] estimate
- Contains robust detection of higher order Balmer and Pa lines
- Sanders+24 demonstrates different nebular attenuation curve in z=4.411 starburst galaxy

3.Nebular reddening

Normalized line ratio "R" can be translated in to E(B-V) assuming Galactic curve
=> ~half has larger E(B-V) for Balmer than Pa lines

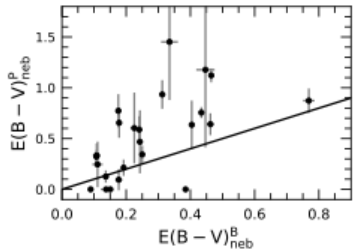

Figure 7. Comparison of $E(B-V)^{B}_{neb}$ and $E(B-V)^{P}_{neb}$ for the 24 galaxies in the final sample. The line of equality is indicated in black.

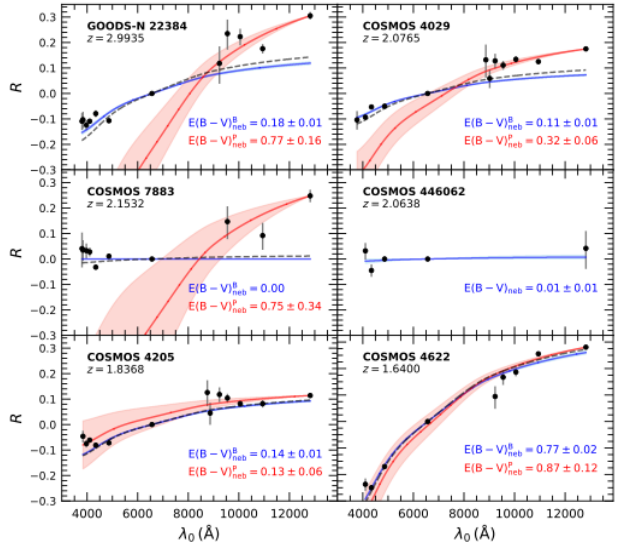

Figure 6. R versus rest-frame wavelength for a representative subsample of 6 galaxies. The measured values and uncertainties in R are

4.Effective Attenuation Curve

Steeper attenuation curve at NIR
⇒ Average curve (0.35-1.28um):

$$\langle k'_{\rm neb}(\lambda)\rangle = -14.198 + \frac{17.002}{\lambda/\mu{\rm m}} - \frac{8.086}{(\lambda/\mu{\rm m})^2} + \frac{2.177}{(\lambda/\mu{\rm m})^3} - \frac{0.319}{(\lambda/\mu{\rm m})^4} + \frac{0.021}{(\lambda/\mu{\rm m})^5}, \quad (11)$$

⇒ Rv=2.3~14.2 (Median 5.5)

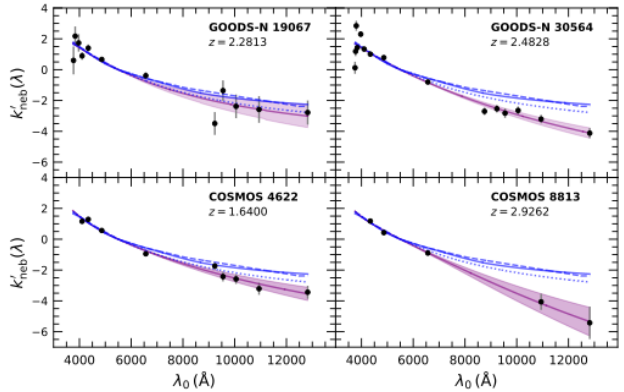

Figure 8. $k'_{neb}(\lambda)$ versus λ_0 for four galaxies in the sample, with the best-fit fifth-order polynomials and 1σ confidence intervals shown by the

5 .Discussion

Large Rv can be explained by geometry of dust around OB associations.
=> Covering fraction (fcov) model can explain Figure 6.

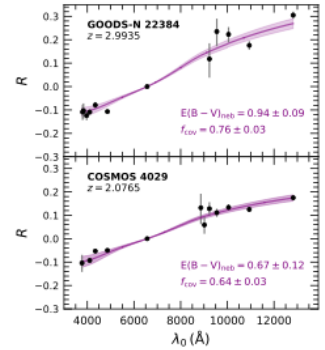

Figure 15. R versus rest-frame wavelength for two galaxies in the

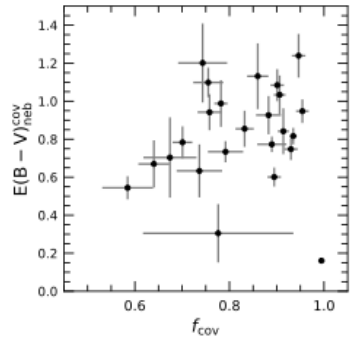

Figure 16. Distribution of f_{cov} and $E(B-V)^{cov}_{neb}$ for the full sample

- Rv correlates with fcov
- High Rv is accompanied by lower fcov and higher E(B-V)neb
- Supporting that young star-forming galaxies has flatter attenuation curve (and higher Rv)

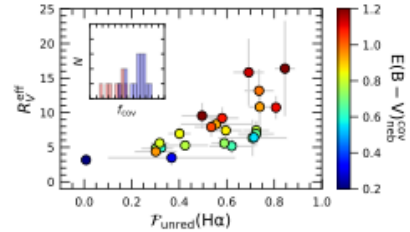

Figure 20. R_V^{eff} as a function of the unreddened fraction of light

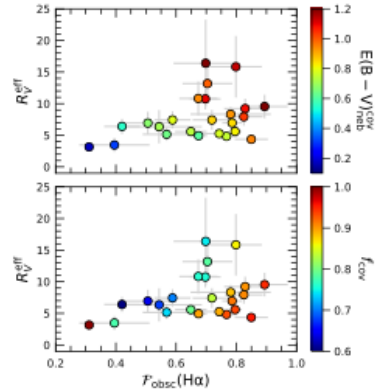

Figure 21. R_V^{eff} as a function of the fraction of dust-obscured Hα